Administration Routes for SSTR-/PSMA- and FAP-Directed Theranostic Radioligands in Mice

Jasmin M. Klose[1], Jasmin Wosniack[1], Janette Iking[1], Magdalena Staniszewska[1], Fadi Zarrad[1], Marija Trajkovic-Arsic[2,3], Ken Herrmann[1], Pedro Fragoso Costa[1], Katharina Lueckerath[1,4], and Wolfgang P. Fendler[1]

[1]Department of Nuclear Medicine, University Hospital Essen, University of Duisburg–Essen, Essen, Germany; [2]Division of Solid Tumor Translational Oncology, German Cancer Consortium, West German Cancer Center, University Hospital Essen, Essen, Germany; [3]German Cancer Consortium and German Cancer Research Center, Heidelberg, Germany; and [4]Ahmanson Translational Theranostics Division, Department of Molecular and Medical Pharmacology, David Geffen School of Medicine, UCLA, Los Angeles, California

The NETTER-1, VISION, and TheraP trials proved the efficacy of repeat intravenous application of small radioligands. Application by subcutaneous, intraperitoneal, or oral routes is an important alternative and may yield comparable or favorable organ and tumor radioligand uptake. Here, we assessed organ and tumor biodistribution for various radioligand application routes in healthy mice and models of cancer expressing somatostatin receptor (SSTR), prostate-specific membrane antigen (PSMA), and fibroblast activation protein (FAP). **Methods:** Healthy and tumor-bearing male C57BL/6 or NOD SCID γ-mice, respectively, were administered a mean of 6.0 ± 0.5 MBq of ^{68}Ga-DOTATOC (RM1-SSTR allograft), 5.3 ± 0.3 MBq of ^{68}Ga-PSMA11 (RM1-PSMA allograft), or 4.8 ± 0.2 MBq of ^{68}Ga-FAPI46 (HT1080-FAP xenograft) by intravenous, intraperitoneal, subcutaneous, or oral routes. In vivo PET images and ex vivo biodistribution in tumor, organs, and the injection site were assessed up to 5 h after injection. Healthy mice were monitored for up to 7 d after the last scan for signs of stress or adverse reactions. **Results:** After intravenous, intraperitoneal, and subcutaneous radioligand administration, average residual activity at the injection site was less than 17 percentage injected activity per gram (%IA/g) at 1 h after injection, less than 10 %IA/g at 2 h after injection, and no more than 4 %IA/g at 4 h after injection for all radioligands. After oral administration, at least 50 %IA/g remained within the intestines until 4 h after injection. Biodistribution in organs of healthy mice was nearly equivalent after intravenous, intraperitoneal, and subcutaneous application at 1 h after injection and all subsequent time points (≤1 %IA/g for liver, blood, and bone marrow; 11.2 ± 1.4 %IA/g for kidneys). In models for SSTR-, PSMA- and FAP-expressing cancer, tumor uptake was increased or equivalent for intraperitoneal/subcutaneous versus intravenous injection at 5 h after injection (ex vivo): SSTR, 7.2 ± 1.0 %IA/g (P = 0.0197)/6.5 ± 1.3 %IA/g (P = 0.0827) versus 2.9 ± 0.3 %IA/g, respectively; PSMA, 3.4 ± 0.8 %IA/g (P = 0.9954)/3.9 ± 0.8 %IA/g (P = 0.8343) versus 3.3 ± 0.7% IA/g, respectively; FAP, 1.1 ± 0.1 %IA/g (P = 0.9805)/1.1 ± 0.1 %IA/g (P = 0.7446) versus 1.0 ± 0.2 %IA/g, respectively. **Conclusion:** In healthy mice, biodistribution of small theranostic ligands after intraperitoneal/subcutaneous application is nearly equivalent to that after intravenous injection. Subcutaneous administration resulted in the highest absolute SSTR tumor and tumor-to-organ uptake as compared with the intravenous route, warranting further clinical assessment.

Received Oct. 29, 2021; revision accepted Dec. 28, 2021.

For correspondence or reprints, contact Wolfgang P. Fendler (wolfgang.fendler@uk-essen.de).

Published online Jan. 6, 2022.

Key Words: radioligand; biodistribution; small-animal PET; theranostic; intravenous; subcutaneous

J Nucl Med 2022; 63:1357–1363
DOI: 10.2967/jnumed.121.263453

NETTER-1 (*1*), and the more recent clinical trials TheraP (*2*) and VISION (*3*), established somatostatin receptor (SSTR)– and prostate-specific membrane antigen (PSMA)–directed small-ligand radiotheranostics as efficacious cancer therapy with favorable safety profiles. Recently, fibroblast activation protein (FAP)–targeting small ligands have emerged for PET and therapy of cancers (*4*). Intravenous application is the standard route for radioligands. However, oral, intraperitoneal, and subcutaneous administrations are faster and require a lower level of training than does intravenous administration, both in the preclinical and in the clinical settings. The volume of preclinical and clinical radioligand applications is growing rapidly, and thus, there is an urgent unmet need to assess alternative application routes to address the increasing demand. In addition, the field of FAP-directed therapies is dynamic and evolving, highlighting the emerging need for optimization of administration routes for these novel radioligands for ongoing preclinical and clinical assessment. With this intent, assessment of biodistribution and administration routes for ^{68}Ga-FAPI46 (FAP inhibitor [FAPI]) was requested by the German Federal Institute for Drugs and Medical Devices for recent approval of a prospective clinical trial on ^{68}Ga-FAPI46 PET/CT for various types of cancer (NCT04571086).

We hypothesized that intraperitoneal/subcutaneous application would yield organ and tumor biodistribution nearly equivalent to that of the routine intravenous injection. We further hypothesized that organ and tumor uptake would be significantly lower after oral application of radioligands. Here, we compare tumor and organ biodistribution after intravenous, intraperitoneal, subcutaneous, and oral application of small radioligands in healthy mice and mouse models of SSTR-, PSMA-, and FAP-expressing cancer.

MATERIALS AND METHODS

Cell Culture

RM1 cells, virally stably transduced with SFG-Egfp/Luc (RM1-PGLS) or pMSCV-IRES-YFP II-hSSTR (RM1-SSTR) to express high levels of cell surface human PSMA or SSTR2 (*5*), were obtained from

Johannes Czernin (UCLA). HT1080-FAP cells were a gift from Uwe Haberkorn (University Hospital of Heidelberg). HT1080 cells were stably transfected with the plasmid pcDNAI/neo-FAP (expressing the untagged full-length complementary DNA of human FAP) followed by neomycin selection (*6*). RM1-PSMA and RM1-SSTR were maintained in RPMI 1640 medium (GIBCO) and HT1080-FAP in Dulbecco modified Eagle medium (GIBCO), both with 10% fetal bovine serum (Thermo Fisher Scientific) and with 0.5% penicillin/streptomycin (GIBCO), at 37°C with 5% CO_2. Cells were thawed for 2 wk or passaged 3 times before inoculation. Cells were routinely assessed for *Mycoplasma* contamination using the VenorGeM OneStep kit (Minerva Biolabs).

Radiosynthesis

^{68}Ga-DOTATOC, ^{68}Ga-PSMA11, and ^{68}Ga-FAPI46 were obtained from the radiopharmacy of our clinic. Clinical-grade radiolabeling of precursors (DOTATOC, PSMA11, FAPI46) was performed using the Modular-Lab eazy for DOTATOC and PSMA or Scintomics GRP 3V for FAPI using commercially available reagent kits. The final solution had less than 5 μg/mL for ^{68}Ga-DOTATOC, less than 3 μg/mL for ^{68}Ga-PSMA, and approximately 50 μg/mL for ^{68}Ga-FAPI, with a 100-μL injected volume per mouse. Radiochemical purity was determined with radio–high-performance liquid chromatography (FAPI: Chromolith Performance RP18e column from Merck [100 × 3 mm], gradient of 0%–20% MeCN + 0.1% trifluoroacetic acid in 5 min, run time of 15 min; PSMA: 5%–40% MeCN + 0.1% trifluoroacetic acid in 10 min, run time of 15 min; DOTATOC: 24% MeCN + 0.1% trifluoroacetic acid for 8 min, then 24%–60% in 1 min, run time of 15 min; and instant thin-layer chromatography–silica gel [ammonium acetate, 77 g/L, and methanol R, 50:50 v/v]). The radiochemical purity exceeded 98% for all radioligands.

Mice and Tumor Models

Male C57BL/6 and NOD SCID Gamma mice were purchased from Charles River Laboratories (6–8 wk old) and housed under specific pathogen-free conditions with food and water available ad libitum. The health status of the mice was monitored by assessing a summarized score twice a week (healthy animals) or daily (tumor-bearing animals). The study was approved by the North Rhine–Westphalia State Agency for Nature, Environment, and Consumer Protection, Germany (permit AZ.81-02.04.2018.A090).

For subcutaneous tumors, 0.1×10^6 RM1-SSTR or RM1-PSMA (C57BL/6) cells or 1.0×10^6 HT1080-FAP (NOD SCID Gamma) cells in Matrigel (Corning)/phosphate-buffered saline (50:50 ratio) were injected into the shoulder region of the mice. Tumor volume (V) was calculated by measuring the length (L) and width (W) of tumors by caliper and using the formula $V = {}^1/_2(L \times W^2)$ (*7*). PET scans were acquired 7–10 d after tumor inoculation, as described previously (*5,8*). Mean (+SEM) tumor volumes were 0.39 ± 0.09 cm^3 (interquartile range, 0.07–0.66 cm^3) for RM1-SSTR tumors, 0.05 ± 0.01 cm^3 (interquartile range, 0.02–0.08 cm^3) for RM1-PSMA tumors, and 0.22 ± 0.03 cm^3 (interquartile range, 0.06–0.25 cm^3) for HT1080-FAP tumors.

Radioligand Application and Small-Animal PET/CT

Healthy or tumor-bearing anesthetized mice (1.5%–2% isoflurane) received a mean of 6.0 ± 0.5 MBq of ^{68}Ga-DOTATOC, 5.3 ± 0.3 MBq of ^{68}Ga-PSMA11, or 4.8 ± 0.2 MBq of ^{68}Ga-FAPI46 intravenously (tail vein), intraperitoneally, subcutaneously, or orally (oral HT1080-FAP tumor-bearing mice only) (differences between injected activities were not statistically significant). Each healthy mouse received intravenous, intraperitoneal, subcutaneous, and oral administration, with a 1-wk

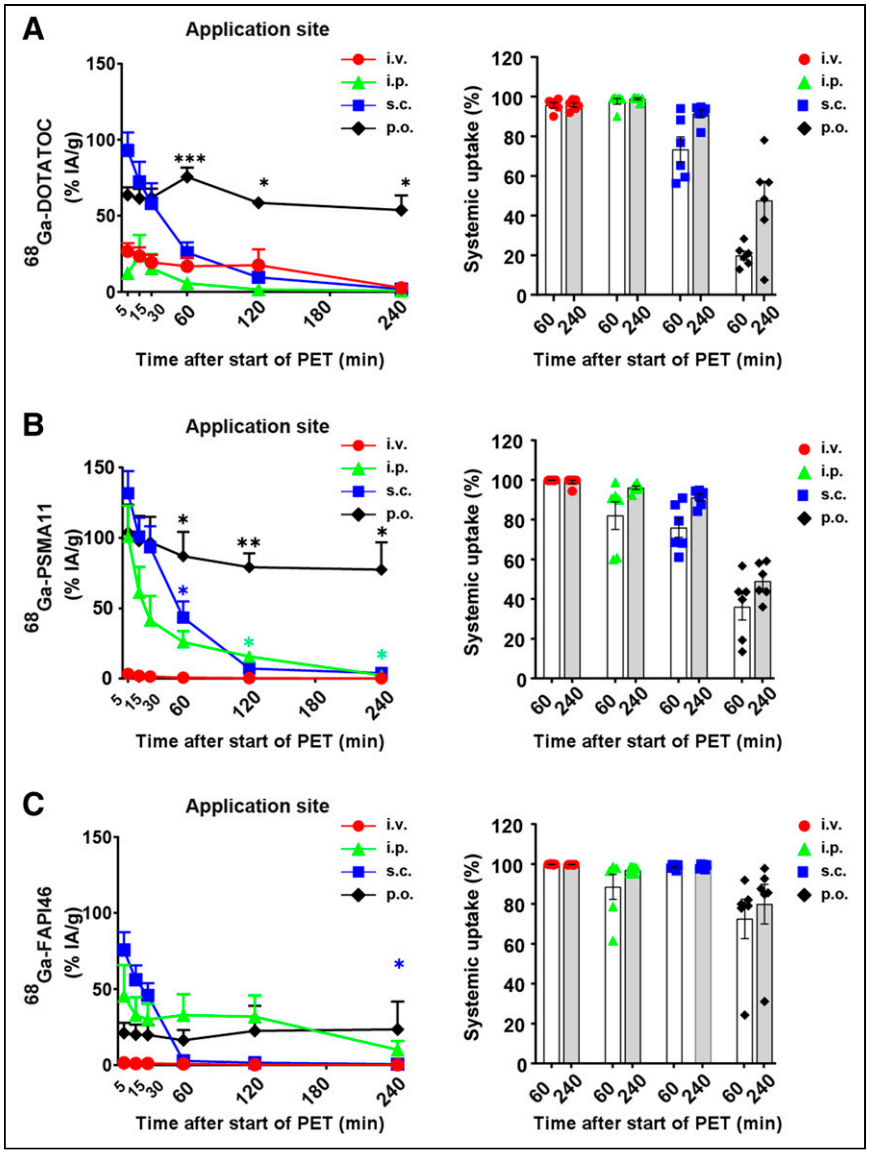

FIGURE 1. Activity at application site and systemic availability over time in healthy mice. Retention of ^{68}Ga-DOTATOC (A), ^{68}Ga-PSMA11 (B), and ^{68}Ga-FAPI46 (C) is shown in healthy mice (6/group) at application site. (Left) Time–activity curves illustrate radioligand dynamics at application site for intravenous, intraperitoneal, subcutaneous, and oral application. (Right) Relative systemic uptake of whole-body VOI excluding application site VOI is displayed as percentage total-body uptake. Each dot represents a mouse. Data are mean + SEM. i.p. = intraperitoneal; i.v. = intravenous; p.o. = oral; s.c. = subcutaneous. *$P < 0.05$ compared with intravenous application. **$P < 0.01$ compared with intravenous application. ***$P < 0.001$ compared with intravenous application.

interval between PET/CT scans (Supplemental Fig. 1A; supplemental materials are available at http://jnm.snmjournals.org). Each tumor-bearing mouse was scanned twice, at 1 and 4 h after injection, after either intravenous, intraperitoneal, or subcutaneous application and was sacrificed at about 5 h after injection for ex vivo analysis (Supplemental Fig. 1B). Imaging was performed with a β-CUBE (PET) and X-CUBE (CT) (Molecubes) in temperature-controlled beds with monitoring of breathing frequency. PET/CT was performed (PET, 15 min; CT, 5 min) in list mode with frames for 5, 10, and 15 min (dynamic scans; maximum delay between injection and scan start, 5 min) and static scans at 1, 2, and 4 h after injection for healthy mice and 1 and 4 h after injection for tumor groups.

Image Reconstruction and Processing

Images were reconstructed using an iterative image space reconstruction algorithm (30 iterations) with attenuation correction of the corresponding CT image. PET data were reconstructed into a 192 × 192 transverse matrix, producing a 400-μm isometric voxel size. PET images were evaluated with PMOD software (PMOD Technologies LLC). Decay-corrected mean percentage injected activity per gram (%IA/g) of the tumor and organs of interest was derived from DICOM images. Volumes of interest (VOIs) were defined as spheres with a diameter of 5 mm (lung, liver, spleen, intestines, heart, brain, kidneys) and 2.5 mm (bone marrow, thigh muscle, blood pool, injection site, tumor) in tissues of interest. %IA/g was calculated from the average pixel values reported in Bq/mL within these VOIs corrected for radioactive decay and mouse body weight.

Ex Vivo Analysis

Approximately 5 h after injection, the animals were killed and organs of interest were extracted, dabbed dry, weighed, and measured for radioactivity in an automated γ-counter (Perkin-Elmer γ-Counter 2480 Wizard^2). Organ and tumor uptake was calculated from radioactive counts, decay-corrected, and expressed as %IA/g.

Data and Statistical Analysis

Data are presented as mean ± SEM unless indicated otherwise. All statistical analyses were performed using GraphPad Prism (version 9.1.0; GraphPad Software). Tumor-to-organ uptake ratios were calculated for blood, kidney, liver, and bone marrow (femur) using %IA/g at 1 h and 4 h in in vivo VOIs and at 5 h for ex vivo γ-counter measurements (%IA/g tumor/%IA/g organ). Statistical significance was assessed using the Brown–Forsythe and Welch ANOVA test with the Dunnett T3 multiple-comparisons test or the Tukey multiple-comparisons test. *P* values below 0.05 were considered statistically significant.

RESULTS

Local and Systemic Activity

To assess the biodistribution of radioligands applied via different routes, we measured the activity retained at the injection site versus the overall systemic activity distribution excluding the application site. Activity at the injection site decreased over time after intravenous, intraperitoneal, and subcutaneous administration in healthy mice (Fig. 1; Supplemental Fig. 1). For all radioligands, mean residual activity at the injection site 4 h after injection was 1.0 ± 0.3 %IA/g for intravenous, 4.4 ± 2.1 %IA/g for intraperitoneal, and 2.1 ± 0.5 %IA/g for subcutaneous; this correlated inversely with increased systemic availability of radioligands. Oral administration resulted in significant and prolonged retention of radioligands in the stomach and proximal small bowel as well as a low systemic distribution (Figs. 1A–1C). After oral administration, average systemic uptake was highest for ^{68}Ga-FAPI46 (Fig. 1C). Therefore, oral application was further explored in HT1080-FAP tumor-bearing mice.

Near-Equivalent Organ Biodistribution of Radioligands After Intraperitoneal, Subcutaneous, and Intravenous Application in Healthy Mice

In healthy mice, intraperitoneal, subcutaneous, and intravenous injection of radioligands resulted in near-equivalent organ biodistribution in vivo (Figs. 2–4; Supplemental Figs. 2 and 3). Radioligand retention in blood and kidney is listed in Supplemental Table 1. Blood retention in healthy mice was significantly higher after intraperitoneal/subcutaneous than after intravenous application of ^{68}Ga-PSMA11 (intraperitoneal: $P = 0.0226$ at 1 h, 0.0463 at 2 h, and 0.0394 at 4 h; subcutaneous: $P = 0.0880$ at 1 h, 0.0021 at 2 h, and 0.065 at 4 h). For ^{68}Ga-DOTATOC and ^{68}Ga-FAPI46, blood and kidney distribution after intraperitoneal/subcutaneous application were comparable to those after intravenous injection (Figs. 2–4). In further organs, including liver, bone marrow, lung, heart, spleen, intestines, brain, and muscle, the intraperitoneal, subcutaneous, and intravenous application routes exhibited comparable physiologic biodistribution (Supplemental Fig. 2). Moreover, in healthy mice, no short-term or longer-term adverse effects of radioligand application and PET/CT procedures were noted during the study duration (5 wk).

Increased or Comparable Tumor Uptake After Intraperitoneal/Subcutaneous Versus Intravenous Injection of Radioligands

To evaluate the impact of the application route on tumor uptake of ^{68}Ga-DOTATOC, ^{68}Ga-PSMA11, or ^{68}Ga-FAPI46, we assessed in vivo and ex vivo tumor and organ uptake in SSTR-, PSMA- and

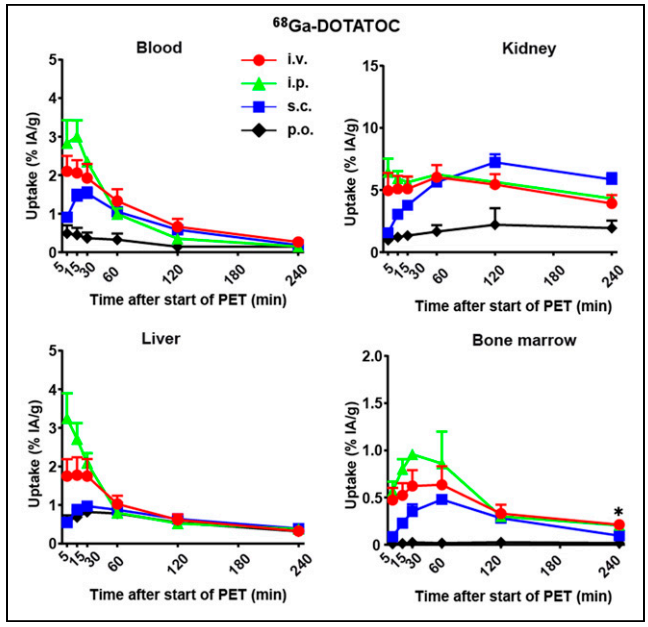

FIGURE 2. In healthy mice, organ biodistribution at ≥1 h after intraperitoneal/subcutaneous radioligand application is nearly equivalent to that after intravenous injection. Healthy mice (6/group) underwent PET after intravenous, intraperitoneal, subcutaneous, and oral radioligand application at minutes 0–30 after start of PET and after 1, 2, and 4 h and were subsequently killed. Time–activity curves illustrate in vivo PET biodistribution of ^{68}Ga-DOTATOC dynamics in VOIs at indicated times for intravenous, intraperitoneal, subcutaneous, and oral application. Data are mean + SEM. i.p. = intraperitoneal; i.v. = intravenous; p.o. = oral; s.c. = subcutaneous. *$P < 0.05$ compared with intravenous injection.

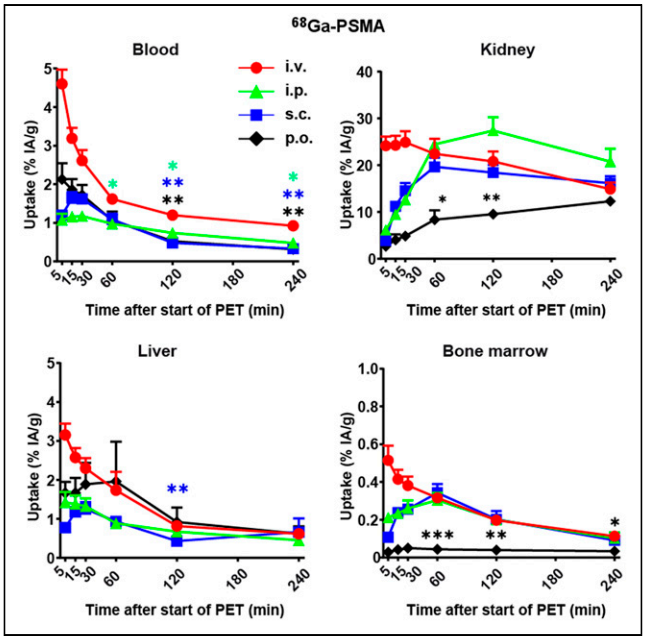

FIGURE 3. In healthy mice, organ biodistribution at ≥1 h after intraperitoneal/subcutaneous radioligand application is nearly equivalent to that after intravenous injection. Healthy mice (6/group) underwent PET after intravenous, intraperitoneal, subcutaneous, and oral radioligand application at minutes 0–30 after start of PET and after 1, 2, and 4 h and were subsequently killed. Time–activity curves illustrate in vivo PET biodistribution of ^{68}Ga-PSMA dynamics in VOIs at indicated times for intravenous, intraperitoneal, subcutaneous, and oral application. Data are mean + SEM. i.p. = intraperitoneal; i.v. = intravenous; p.o. = oral; s.c. = subcutaneous. *$P < 0.05$ compared with intravenous injection. **$P < 0.01$ compared with intravenous injection. ***$P < 0.001$ compared with intravenous injection.

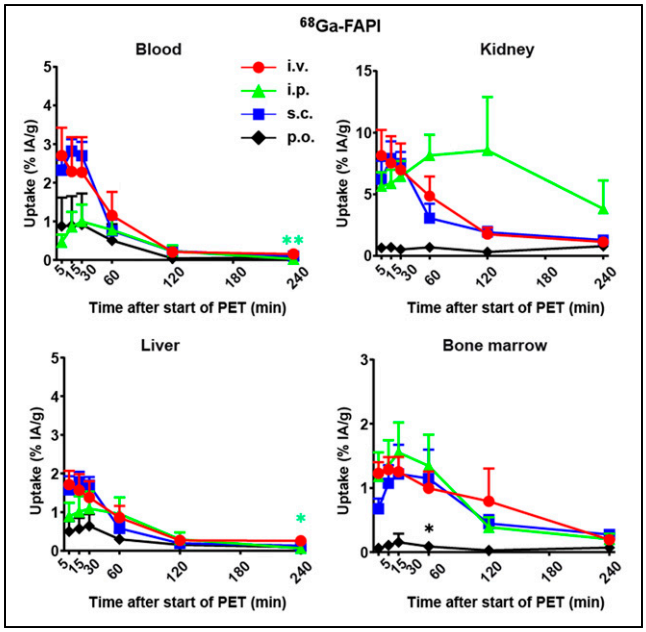

FIGURE 4. In healthy mice, organ biodistribution at ≥1 h after subcutaneous radioligand application is nearly equivalent to that after intravenous injection. Healthy mice (6/group) underwent PET scans after intravenous, intraperitoneal, subcutaneous, and oral radioligand application at minutes 0–30 after start of PET and after 1, 2, and 4 h and were subsequently killed. Time–activity curves illustrate in vivo PET biodistribution of ^{68}Ga-FAPI dynamics in VOIs at indicated times for intravenous, intraperitoneal, subcutaneous, and oral application. Data are mean + SEM. i.p. = intraperitoneal; i.v. = intravenous; p.o. = oral; s.c. = subcutaneous. *$P < 0.05$ compared with intravenous injection. **$P < 0.01$ compared with intravenous injection.

FAP-expressing tumor models (Table 1; Figs. 5–7; Supplemental Figs. 4 and 5).

In mice bearing SSTR tumors, intraperitoneal/subcutaneous application resulted in significantly higher mean tumor uptake than did intravenous application: $P = 0.0124$ and 0.0377, respectively, at 1 h; $P = 0.0301$ and 0.0411, respectively, at 4 h; and $P = 0.0197$ and 0.0827, respectively, at 5 h [ex vivo]) (Table 1; Supplemental Fig. 4). Tumor uptake of ^{68}Ga-PSMA11 or ^{68}Ga-FAPI46 after intraperitoneal/subcutaneous injection in mice bearing PSMA- or FAP-expressing tumors was comparable to the uptake observed after intravenous injection (Table 1).

Oral administration in mice bearing FAP-expressing tumors did not result in notable tumor uptake (Table 1; Supplemental Fig. 4). Oral application of ^{68}Ga-FAPI46 in tumor-bearing mice yielded biodistribution characteristics comparable to those seen in healthy mice (Supplemental Fig. 4), with high gastrointestinal retention of the radioligand and low systemic distribution.

Tumor-to-organ uptake ratios of organs relevant to dosimetry (*9,10*) for intraperitoneal/subcutaneous versus intravenous application are depicted in Figures 5–7. Intraperitoneal/subcutaneous application resulted in increased or equivalent tumor-to-liver ratios at 5 h after injection when compared with intravenous (mean ratio 5 h after injection): ^{68}Ga-DOTATOC: 27.4 ± 2.2-fold ($P = 0.0138$)/25.3 ± 5.6-fold ($P = 0.2756$) versus 13.9 ± 2.9-fold, respectively; ^{68}Ga-PSMA11: 28.2 ± 7.4-fold ($P = 0.4504$)/39.4 ± 5.7-fold ($P = 0.0259$) versus 16.9 ± 2.8-fold, respectively; and ^{68}Ga-FAPI46: 6.1 ± 1.6-fold ($P = 0.4198$)/12.0 ± 1.1-fold ($P = 0.0005$) versus 3.7 ± 0.4-fold, respectively (Figs. 5–7). Tumor-to-marrow ratios were higher for intraperitoneal than for intravenous application in mice bearing SSTR-expressing tumors: 50.7 ± 4.3 versus 25.7 ± 4.9, respectively ($P = 0.0096$) (Fig. 5). Subcutaneous application resulted in higher tumor-to-blood ratios than did intravenous application in mice bearing PSMA-expressing tumors: 24.5 ± 4.2-fold versus 6.0 ± 0.9-fold, respectively ($P = 0.0186$). For other tumor-to-organ uptake ratios, no significant difference was observed (Fig. 6). Oral application of ^{68}Ga-FAPI46 resulted in negligible uptake in organs and tumors (Table 1; Supplemental Fig. 4).

DISCUSSION

The current delivery method for radioligands for nuclear imaging or therapy is intravenous injection. However, comparing different application routes is important for the translation of novel FAP ligands and optimization of current clinical protocols for PSMA or SSTR ligands.

The current study aimed at comparing the biodistribution of SSTR-, PSMA-, and FAP-directed small radioligands administered intraperitoneally, subcutaneously, or orally with the standard intravenous application. Alternative application routes may alter systemic distribution and tumor uptake (*11–13*), such as by slowing absorption because of a reduced rate of molecular transport via the lymphatics and blood flow to the organs of interest or tumor (*14*).

Administration of small radioligands intravenously, intraperitoneally, and subcutaneously was feasible and well tolerated as assessed by a scoring system including the behavior and overall physical appearance of mice. Small-radioligand systemic availability and biodistribution were comparable for intraperitoneal/subcutaneous versus intravenous application (Fig. 1–4). In addition,

TABLE 1
Intraperitoneal/Subcutaneous Application Led to Increased or Equivalent Tumor Uptake Compared with Intravenous Injection

Radioligand	IV	IP	SC	PO	*P*		
					IV vs. IP	IV vs. SC	IV vs. PO
RM1-SSTR (^{68}Ga-DOTATOC)							
In vivo, 1 h	5.3 ± 0.6	9.9 ± 1.0	10.8 ± 1.6	NA	0.0124*	0.0377*	NA
In vivo, 4 h	4.4 ± 0.7	8.6 ± 1.1	11.1 ± 2.0	NA	0.0301*	0.0411*	NA
Ex vivo, 5 h	2.9 ± 0.3	7.2 ± 1.1	6.5 ± 1.3	NA	0.0197*	0.0827	NA
RM1-PSMA (^{68}Ga-PSMA11)							
In vivo, 1 h	2.9 ± 0.2	3.0 ± 0.6	2.6 ± 0.4	NA	0.9837	0.8297	NA
In vivo, 4 h	2.6 ± 0.2	2.6 ± 0.7	2.9 ± 0.5	NA	0.9996	0.8289	NA
Ex vivo, 5 h	3.3 ± 0.7	3.4 ± 0.8	3.9 ± 0.8	NA	0.9954	0.8343	NA
HT1080-FAP (^{68}Ga-FAPI46)							
In vivo, 1 h	1.2 ± 0.2	2.0 ± 0.4	2.2 ± 1.1	0.1 ± 0.03	0.3024	0.6732	0.0032†
In vivo, 4 h	1.0 ± 0.2	1.5 ± 0.3	1.1 ± 0.6	0.1 ± 0.04	0.4559	0.9911	0.0087†
Ex vivo, 5 h	1.0 ± 0.2	1.1 ± 0.1	1.4 ± 0.4	0.02 ± 0.01	0.9805	0.7446	0.0058†

*$P < 0.05$.
†$P < 0.01$.
IV = intravenous; IP = intraperitoneal; SC = subcutaneous; PO = oral; NA = not applicable.
Data are mean %IA/g ± SEM of 6 mice per group.

intraperitoneal/subcutaneous administration in mice resulted in significantly higher ^{68}Ga-DOTATOC tumor uptake (Table 1), tumor-to-liver ratio, and tumor-to-marrow ratio in SSTR-expressing tumors than was the case with intravenous injection (Fig. 5).

These findings have implications for preclinical and clinical radioligand administration, since they could offer advantages for both fields. In mice, intravenous injection requires highly trained personnel and is more error-prone (e.g., paravenous injection) and time-consuming. Intraperitoneal/subcutaneous administration may serve as simple alternative application routes for imaging at later time points after injection or therapy, allowing a higher throughput in mouse studies, with lower dropout rates and high reproducibility. In mice, intraperitoneal administration did not compromise radioligand tumor accumulation despite a high initial absorbed dose in the intestines (*15*). However, because of slower systemic bioavailability after intraperitoneal/subcutaneous injection, intravenous application is recommended for early dynamic imaging.

In clinical routine, use of alternatives to intravenous application may improve outpatient care and benefit potential new therapy schemes, allowing repeat radioligand application at short intervals.

In patients, intraperitoneal application is limited by a higher likelihood of infection or abdominal organ damage. However, subcutaneous application is already well established as a standard route for injectable medications in outpatients and has an emerging role in delivery of biotherapeutics and monoclonal antibodies (*16,17*). Indeed, in patients with accidental paravenous infusion of ^{177}Lu-DOTATOC, absorption from the paravenous injection site occurs with a half-life of less than 4 h (Supplemental Fig. 6); this is in line with a short drainage observed after subcutaneous injection in mice. We therefore expect that subcutaneous application in patients would be feasible.

Still, an increased radiation dose to organs such as kidneys, bone marrow, blood, lungs, or liver may limit benefit from intraperitoneal/

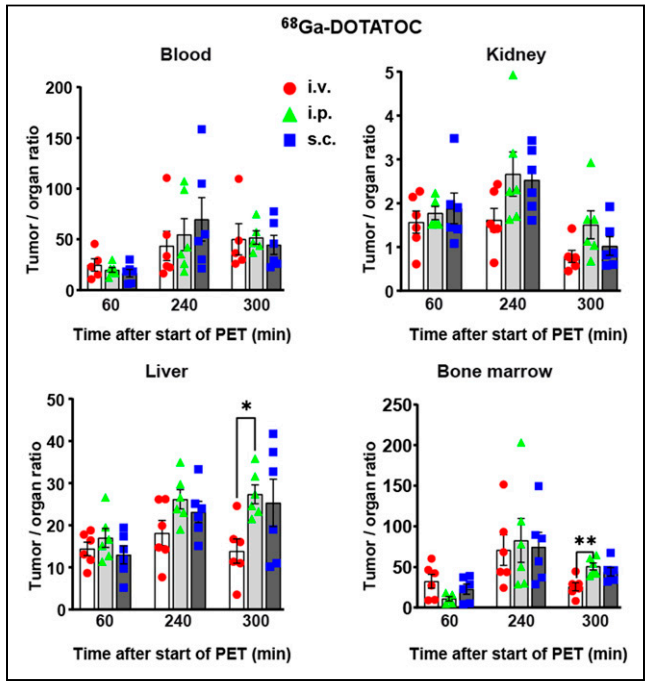

FIGURE 5. Intraperitoneal/subcutaneous radioligand application increases tumor-to-liver uptake compared with intravenous injection. Mice with subcutaneous RM1-SSTR tumors (6/group) received intravenous, intraperitoneal, and subcutaneous administration of ^{68}Ga-DOTATOC; underwent PET after 1 and 4 h; and then were killed (5 h), followed by assessment of radioactivity in organs and tumors by γ-counter. Plots show tumor-to-organ ratios after intravenous, intraperitoneal, and subcutaneous administration of ^{68}Ga-DOTATOC. Each dot represents a mouse. Data are mean ± SEM. i.p. = intraperitoneal; i.v. = intravenous; s.c. = subcutaneous. *$P < 0.05$ compared with intravenous injection. **$P < 0.01$ compared with intravenous injection.

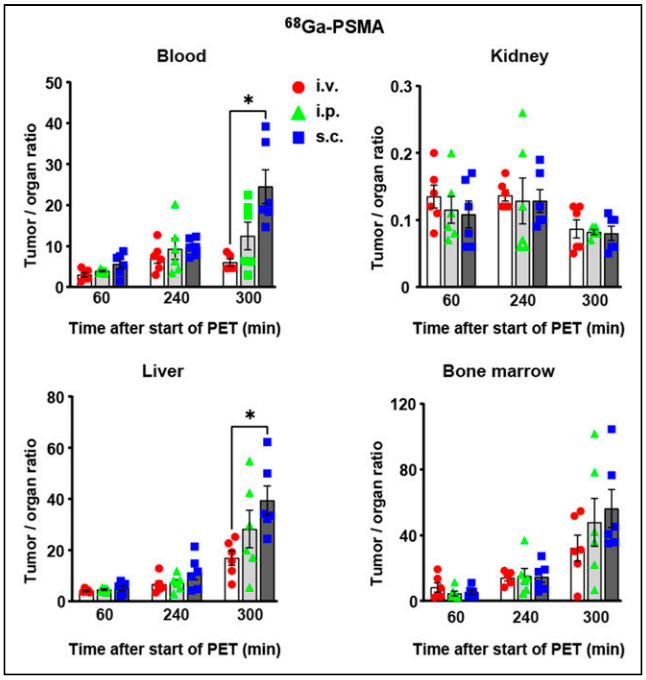

FIGURE 6. Intraperitoneal/subcutaneous radioligand application increases tumor-to-liver uptake compared with intravenous injection. Mice with subcutaneous RM1-PSMA tumors (6/group) received intravenous, intraperitoneal, and subcutaneous administration of ^{68}Ga-PSMA; underwent PET after 1 and 4 h; and then were killed (5 h), followed by assessment of radioactivity in organs and tumors by γ-counter. Plots show tumor-to-organ ratios after intravenous, intraperitoneal, and subcutaneous administration of ^{68}Ga-PSMA. Each dot represents a mouse. Data are mean ± SEM. i.p. = intraperitoneal; i.v. = intravenous; s.c. = subcutaneous. *$P < 0.05$ compared with intravenous injection.

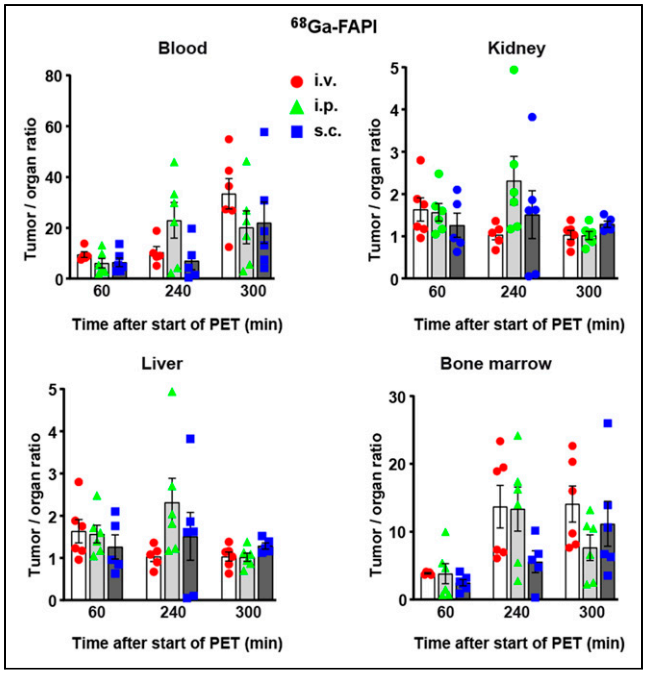

FIGURE 7. Intraperitoneal/subcutaneous radioligand application increases tumor-to-liver uptake compared with intravenous injection. Mice with subcutaneous HT-1080 tumors (6/group) received intravenous, intraperitoneal, and subcutaneous administration of ^{68}Ga-FAPI; underwent PET after 1 and 4 h; and then were killed (5 h), followed by assessment of radioactivity in organs and tumors by γ-counter. Plots show tumor-to-organ ratios after intravenous, intraperitoneal, and subcutaneous administration of ^{68}Ga-FAPI. Each dot represents a mouse. i.p. = intraperitoneal; i.v. = intravenous; s.c. = subcutaneous. Data are mean ± SEM.

subcutaneous injection. However, if radioligand therapy regimens were changed to a weekly or biweekly schedule using subcutaneous application, activities for each administration could probably be reduced in favor of these more frequent treatments. Weekly or biweekly intraperitoneal/subcutaneous application could be realized by outpatient care, reducing the patient's time in the hospital, personnel capacities, and, thus, costs.

In this study, uptake in nontarget tissues did not exceed critical values or radiation dose as suggested from measured uptake in %IA/g (Figs. 2–4). Therefore, we assume that a detrimental radiation burden to organs at risk (mainly kidneys) after intraperitoneal/subcutaneous application when compared with the standard intravenous route is unlikely. Notably, preclinical and clinical studies for DOTA-TOC- and PSMA-targeting radiotherapies demonstrated that after intravenous administration, absorbed doses in organs at risk are not likely to cause relevant radiotoxicity (*9,10,18,19*). However, to precisely estimate the additional absorbed dose to the adjacent tissue (by the intraperitoneal/subcutaneous route) after radioligand therapy, further studies with ^{177}Lu-labeled ligands and quantitative preclinical SPECT imaging should be performed. Yet, if we assume a half-life of 2.3 h for the change in local activity over time at the injection site, as recently published by Tylski et al. (*20*), we would not expect to detect a change in dosimetry between 1 ^{177}Lu administration and, for example, 2–3 administrations spaced by 48 h.

To date, the entire theranostics routine is based on rather conservative application schemes with few possibilities of patient-specific modification. Our observation that subcutaneous application showed similar tumor uptake to intravenous application may open new opportunities for alternative application schemes in the clinical routine—for example, weekly or biweekly applications, which are less feasible if using repeat intravenous injections. Also, subcutaneous application is faster and easier than intravenous and could thus be realized in outpatient care by medical laboratory assistants in a time-efficient manner for both patient and clinic personnel. Furthermore, it would be interesting to investigate the influence of intravenous application rate (applied dose per time) on tumor uptake. This investigation could be realized in a clinical study or observational trial on patients with poor vein status.

This study had some limitations. It assessed ^{68}Ga-ligands for PET imaging and did not examine therapeutic ^{177}Lu-labeled ligands. Furthermore, in-bed injection with concurrent dynamic PET acquisition was not performed, and because of the short ^{68}Ga half-life, time points beyond 5 h after injection were not feasible.

CONCLUSION

In mice, PET imaging after intravenous, intraperitoneal, or subcutaneous injection of SSTR-, PSMA-, or FAP-directed small radioligands is feasible. Intraperitoneal/subcutaneous administration of SSTR-ligands resulted in increased absolute tumor and relative tumor-to-organ uptake compared with intravenous administration, a finding that may translate into improved tumor irradiation in the setting of radioligand therapies and warrants further translational assessment.

DISCLOSURE

This study was funded in part by the Doktor Robert Pfleger-Stiftung, Hallstadt, Germany. Wolfgang Fendler was a consultant for Janssen and Calyx, and he received fees from Bayer and Parexel outside the submitted work. Ken Herrmann reports personal fees from Bayer, Sofie Biosciences, SIRTEX, Adacap, Curium, Endocyte, BTG, IPSEN, Siemens Healthineers, GE Healthcare, Amgen, Novartis, ymabs, Aktis Oncology, Theragnostics, and Pharma15; other fees from Sofie Biosciences; nonfinancial support from ABX; and grants from BTG, outside the submitted work. Katharina Lueckerath reports paid consulting activities for Sofie Biosciences/iTheranostics and funding from AMGEN outside the submitted work. No other potential conflict of interest relevant to this article was reported.

ACKNOWLEDGMENTS

We thank Prof. Dr. Med Uwe Haberkorn for providing HT1080-hFAP cells, and we thank the nuclear medicine team at University Hospital Essen for their support.

KEY POINTS

QUESTION: Are there alternatives to intravenous injection of SSTR-, PSMA-, or FAP-directed radioligands?

PERTINENT FINDINGS: In healthy mice, intraperitoneal/subcutaneous application of small radiotheranostic ligands resulted in near-equivalent systemic availability and organ biodistribution at early (1 h) and late (4 h) time points after injection when compared with intravenous injection. Intraperitoneal/subcutaneous administration significantly increased absolute tumor and relative tumor-to-organ uptake in SSTR tumors (^{68}Ga-DOTATOC) compared with the intravenous route.

IMPLICATIONS FOR PATIENT CARE: Intraperitoneal/subcutaneous application is feasible in animal models of small-radioligand imaging or therapy. Tumor uptake and tolerability of subcutaneous application warrants assessment in clinical studies.

REFERENCES

1. Strosberg J, Wolin E, Chasen B, et al. NETTER-1 phase III in patients with midgut neuroendocrine tumors treated with ^{177}Lu-Dotatate: efficacy and safety results [abstract]. *J Nucl Med.* 2016;57(suppl 2):629.
2. Hofman MS, Emmett L, Sandhu S, et al. [^{177}Lu]Lu-PSMA-617 versus cabazitaxel in patients with metastatic castration-resistant prostate cancer (TheraP): a randomised, open-label, phase 2 trial. *Lancet.* 2021;397:797–804.
3. Sartor O, de Bono J, Chi KN, et al. Lutetium-177-PSMA-617 for metastatic castration-resistant prostate cancer. *N Engl J Med.* 2021;385:1091–1103.
4. Hathi DK, Jones EF. ^{68}Ga FAPI PET/CT: tracer uptake in 28 different kinds of cancer. *Radiol Imaging Cancer.* 2019;1:e194003.
5. Fendler WP, Stuparu AD, Evans-Axelsson S, et al. Establishing ^{177}Lu-PSMA-617 radioligand therapy in a syngeneic model of murine prostate cancer. *J Nucl Med.* 2017;58:1786–1792.
6. Loktev A, Lindner T, Burger EM, et al. Development of fibroblast activation protein-targeted radiotracers with improved tumor retention. *J Nucl Med.* 2019;60:1421–1429.
7. Jensen MM, Jorgensen JT, Binderup T, Kjaer A. Tumor volume in subcutaneous mouse xenografts measured by microCT is more accurate and reproducible than determined by ^{18}F-FDG-microPET or external caliper. *BMC Med Imaging.* 2008;8:16.
8. Lückerath K, Stuparu AD, Wei L, et al. Detection threshold and reproducibility of ^{68}Ga-PSMA11 PET/CT in a mouse model of prostate cancer. *J Nucl Med.* 2018;59:1392–1397.
9. Sandström M, Garske-Roman U, Granberg D, et al. Individualized dosimetry of kidney and bone marrow in patients undergoing ^{177}Lu-DOTA-octreotate treatment. *J Nucl Med.* 2013;54:33–41.
10. Delker A, Fendler WP, Kratochwil C, et al. Dosimetry for ^{177}Lu-DKFZ-PSMA-617: a new radiopharmaceutical for the treatment of metastatic prostate cancer. *Eur J Nucl Med Mol Imaging.* 2016;43:42–51.
11. Strigari L, Konijnenberg M, Chiesa C, et al. The evidence base for the use of internal dosimetry in the clinical practice of molecular radiotherapy. *Eur J Nucl Med Mol Imaging.* 2014;41:1976–1988.
12. Gafita A, Rauscher I, Retz M, et al. Early experience of rechallenge ^{177}Lu-PSMA radioligand therapy after an initial good response in patients with advanced prostate cancer. *J Nucl Med.* 2019;60:644–648.
13. Current K, Meyer C, Magyar CE, et al. Investigating PSMA-targeted radioligand therapy efficacy as a function of cellular PSMA levels and intratumoral PSMA heterogeneity. *Clin Cancer Res.* 2020;26:2946–2955.
14. Sánchez-Félix M, Burke M, Chen HH, Patterson C, Mittal S. Predicting bioavailability of monoclonal antibodies after subcutaneous administration: open innovation challenge. *Adv Drug Deliv Rev.* 2020;167:66–77.
15. Dou S, Smith M, Wang Y, Rusckowski M, Liu G. Intraperitoneal injection is not always a suitable alternative to intravenous injection for radiotherapy. *Cancer Biother Radiopharm.* 2013;28:335–342.
16. Bittner B, Richter W, Schmidt J. Subcutaneous administration of biotherapeutics: an overview of current challenges and opportunities. *BioDrugs.* 2018;32:425–440.
17. Viola M, Sequeira J, Seica R, et al. Subcutaneous delivery of monoclonal antibodies: how do we get there? *J Control Release.* 2018;286:301–314.
18. Wehrmann C, Senftleben S, Zachert C, Muller D, Baum RP. Results of individual patient dosimetry in peptide receptor radionuclide therapy with ^{177}Lu DOTA-TATE and ^{177}Lu DOTA-NOC. *Cancer Biother Radiopharm.* 2007;22:406–416.
19. Kabasakal L, AbuQbeitah M, Aygun A, et al. Pre-therapeutic dosimetry of normal organs and tissues of ^{177}Lu-PSMA-617 prostate-specific membrane antigen (PSMA) inhibitor in patients with castration-resistant prostate cancer. *Eur J Nucl Med Mol Imaging.* 2015;42:1976–1983.
20. Tylski P, Pina-Jomir G, Bournaud-Salinas C, Jalade P. Tissue dose estimation after extravasation of ^{177}Lu-DOTATATE. *EJNMMI Phys.* 2021;8:33.